Article

Charge-Transfer-to-Solvent-Driven Dissolution Dynamics of I(HO)$_n^-$ upon Excitation: Excited-State ab Initio Molecular Dynamics Simulations

Maciej Koaski, Han Myoung Lee, Chaeho Pak, and Kwang S. Kim

J. Am. Chem. Soc., **2008**, 130 (1), 103-112 • DOI: 10.1021/ja072427c

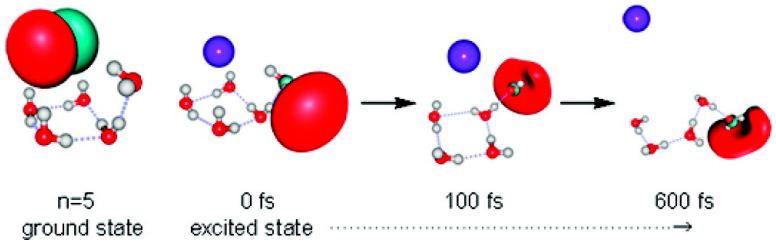

J|A|C|S
ARTICLES
Published on Web 12/11/2007

Charge-Transfer-to-Solvent-Driven Dissolution Dynamics of $I^-(H_2O)_{2-5}$ upon Excitation: Excited-State ab Initio Molecular Dynamics Simulations

Maciej Kołaski,† Han Myoung Lee, Chaeho Pak, and Kwang S. Kim*

Department of Chemistry, Center for Superfunctional Materials, Pohang University of Science and Technology, San 31, Hyojadong, Namgu, Pohang 790-784, Korea

Received April 6, 2007; E-mail: kim@postech.ac.kr

Abstract: In contrast to the extensive theoretical investigation of the solvation phenomena, the dissolution phenomena have hardly been investigated theoretically. Upon the excitation of hydrated halides, which are important substances in atmospheric chemistry, an excess electron transfers from the anionic precursor (halide anion) to the solvent and is stabilized by the water cluster. This results in the dissociation of hydrated halides into halide radicals and electron-water clusters. Here we demonstrate the charge-transfer-to-solvent (CTTS)-driven femtosecond-scale dissolution dynamics for $I^-(H_2O)_{n=2-5}$ clusters using excited state (ES) ab initio molecular dynamics (AIMD) simulations employing the complete-active-space self-consistent-field (CASSCF) method. This study shows that after the iodine radical is released from $I^-(H_2O)_{n=2-5}$, a simple population decay is observed for small clusters ($2 \leq n \leq 4$), while rearrangement to stabilize the excess electron to an entropy-driven structure is seen for $n = 5$. These results are in excellent agreement with the previous ultrafast pump−probe experiments. For the first ~30 fs of the simulations, the iodine plays an important role in rearranging the hydrogen orientations (although the water network hardly changes), which increases the kinetic energy of the cluster. However, ~50 fs after the excitation, the role of the iodine radical is no longer significant. After ~100 fs, the iodine radical is released, and the solvent molecules rearrange themselves to a lower free energy structure. The CTTS-driven dissolution dynamics could be useful in designing the receptors which are able to bind and release ions in host−guest chemistry.

1. Introduction

The nanoscopic details of ion−water cluster interactions[1−4] are important for understanding solvation phenomena in chemical processes,[5−8] designing efficient ionophores/receptors for biological molecular recognition,[9] and engineering self-assembled nanomaterials which involves the interaction with ions.[10,11] Recently, interfacial hydrated halide anions (in particular, iodide) on the surface of the sea are considered to have a significant effect on atmospheric chemistry (such as increasing ozone levels by forming active halogen compounds).[12] Photoexcitation of the halide anion−water clusters usually results in

† Permanent address: Department of Theoretical Chemistry, Institute of Chemistry, University of Silesia, 9 Szkolna Street, 40-006 Katowice, Poland.

(1) (a) Lehr, L.; Zanni, M. T.; Frischkorn, C.; Weinkauf, R.; Neumark, D. M. *Science* **1999**, *284*, 635. (b) Davis, A. V.; Zanni, M. T.; Weinkauf, R.; Neumark, D. M. *Chem. Phys. Lett.* **2002**, *353*, 455. (c) Szpunar, D. E.; Kammrath, K. E.; Faulhaber, A. E.; Neumark, D. M. *J. Chem. Phys.* **2006**, *124*, 054318.
(2) (a) Robertson, W. H.; Diken, E. G.; Price, E. A.; Shin, J.-W.; Johnson, M. A. *Science* **2003**, *299*, 1367. (b) Robertson, W. H.; Johnson, M. A. *Science* **2002**, *298*, 69.
(3) (a) Ghosal, S.; Hemminger, J. C.; Bluhm, H.; Mun, B. S.; Hebenstreit, E. L. D.; Ketteler, G.; Ogletree, D. F.; Requejo, F. G.; Salmeron, M. *Science* **2005**, *307*, 563. (b) Patwari, G. N.; Lisy, J. M. *J. Chem. Phys.* **2003**, *118*, 8555. (c) Kim, K. S.; Tarakeshwar, P.; Lee, J. Y. *Chem. Rev.* **2000**, *100*, 4145. (d) Hurley, S. M.; Dermota, T. E.; Hydutsky, D. P.; Castleman, A. W. *Science* **2002**, *298*, 202.
(4) (a) Singh, N. J.; Olleta, A. C.; Anupriya Park, M.; Yi, H.-B.; Bandyopadhyay, I.; Lee, H. M.; Tarakeshwar, P.; Kim, K. S. *Theor. Chem. Acc.* **2006**, *115*, 127. (b) Singh, N. J.; Park, M.; Min, S. K.; Suh, S. B.; Kim, K. S. *Angew. Chem., Int. Ed.* **2006**, *45*, 3795.(c) Lee, H. M.; Tarakeshwar, P.; Park, J. W.; Kołaski, M. R.; Yoon, Y. J.; Yi, H.-B.; Kim, W. Y.; Kim, K. S. *J. Phys. Chem. A* **2004**, *108*, 2949.
(5) (a) Marcus, Y. *Ion Solvation*, Wiley: Chichester U.K. 1985. (b) Kirk, K. L. *Biochemistry of Halogens and Inorganic Halides*, Plenum: New York 1991. (c) Richens, D. T. *The Chemistry of Aqua Ions*, Wiley: Chichester U.K. 1997. (d) Lisy, J. M. *Int. Rev. Phys. Chem.* **1997**, *16*, 267. (e) Castelman, A. W. *Adv. Gas-Phase Ion Chem.* **1998**, *3*, 185. (f) Coe, J. V. *Int. Rev. Phys. Chem.* **2001**, *20*, 33.
(6) (a) Rodgers, M. T.; Armentrout, P. B. *J. Phys. Chem. A* **1997**, *101*, 1238.-(b) Stace, A. J. *Science* **2001**, *294*, 1292.
(7) (a) Kim, J.; Lee, S.; Cho, S. J.; Mhin, B. J.; Kim, K. S. *J. Chem. Phys.* **1995**, *102*, 839. (b) Kumar, A.; Park, M.; Huh, J. Y.; Lee, H. M.; Kim, K. S. *J. Phys. Chem. A.* **2006**, *110*, 12484. (c) Olleta, A. C.; Lee, H. M.; Kim, K. S. *J. Chem. Phys*. **2007**, *126*, 144311.
(8) (a) Re, S.; Osamura, Y.; Suzuki, Y.; Schaefer, III, H. F. *J. Chem. Phys.* **1998**, *109*, 973. (b) Blake, T. A.; Sharpe, S. W.; Xantheas, S. S. *J. Chem. Phys.* **2000**, *113*, 707. (c) Al-Halabi, A. S.; Bianco, R.; Hynes, J. T. *J. Phys. Chem, A* **2002**, *106*, 7639. (d) Wei, D.; Truchon, J.-F.; Sirois, S.; Salahub, D. *J. Chem. Phys.* **2002**, *116*, 6028. (e) Odde, S.; Mhin, B. J.; Lee, S.; Lee, H. M.; Kim, K. S. *J. Chem. Phys.* **2004**, *120*, 9524.
(9) (a) Atwood, J. L.; Davis, J. E. D.; MacNicol, D. D.; Vögtle, F.; Lehn, J.-M. *Comprehensive Supramolecular Chemistry*; Elsevier: Amsterdam 1996; Vols. 1−11. (b) Yoon, J.; Kim, S. K.; Singh, N. J.; Kim, K. S. *Chem. Soc. Rev.* **2006**, *35*, 355. (c) Singh, N. J.; Lee, H. M.; Hwang, I.-C.; Kim, K. S. *Supramol. Chem.* **2007**, *19*, 321.
(10) (a) Chellappan, K.; Singh, N. J.; Hwang, I.-C.; Lee, J. W.; Kim,. K. S. *Angew. Chem., Int. Ed.* **2005**, *44*, 2899. (b) Ihm, H.; Yun, S.; Kim, H. G.; Kim, J. K.; Kim, K. S. *Org. Lett.* **2002**, *4*, 2897. (c) Choi, H. S.; Suh, S. B.; Cho, S. J.; Kim, K. S. *Proc. Natl. Acad. Sci. U.S.A.* **1998**, *95*, 12094.
(11) (a) Singh, N. J.; Lee, H. M.; Suh, S. B.; Kim, K. S. *Pure Appl. Chem.* **2007**, *79*, 1057. (b) Hong, B. H.; Bae, S. C.; Lee, C.-W.; Jeong, S.; Kim, K. S. *Science* **2001**, *294*, 348. (c) Hong, B. H.; Lee, J. Y.; Lee, C.-W.; Kim, J. C.; Kim, K. S. *J. Am. Chem. Soc.* **2001**, *123*, 10748.
(12) (a) Knipping, E. M.; Lakin, M. J.; Foster, K. L.; Jungwirth, P.; Tobias, D. J.; Gerber, R. B.; Dabdub, D.; Finlayson-Pitts, B. J. *Science* **2000**, *288*, 301−306. (b) Oum, K. W.; Lakin, M. J.; DeHaan, D. O.; Brauers, T.; Finlayson-Pitts, B. J. *Science* **1998**, *279*, 74.

the transfer of an electron from the anionic precursor to the solvent,[13−18] i.e., the charge-transfer-to-solvent (CTTS) phenomena.[19] This photoexcitation dissociates hydrated halide anions into active free halide radicals and water clusters with an excess electron $[e^-(H_2O)_n]$[20,21] in which the excess electron is stabilized by the electron−dipole (e−μ) interaction with the dipole-driven water cluster. This halide ion detachment mechanism in the photoexcitation-driven dissolution dynamics would be of crucial importance in designing novel dynamic receptors which can selectively bind ions and release them by charge transfer upon the excitation. It should be emphasized that, although the ion capture by ion recognition has been well studied, the ion release has never been exploited despite its extreme importance as the extension of the host−guest chemistry.

The CTTS state is a sensitive probe of local solvent structure formation. The water−water H-bond-making/-breaking of iodide−water clusters has been investigated using IR spectroscopy.[22] Johnson and co-workers[23] have found that $I^-(H_2O)_{2-6}$ complexes undergo the electron transfer from I^- to the network of water molecules. Neumark and co-workers[1] observed a shift to higher vertical detachment energy (VDE) at early pump−probe delays for $e^-(H_2O)_{n=5,6}$. This demonstrates that the clusters comprising up to four water molecules exhibit simple population decay, while the clusters for $n \geq 5$ are involved in complex dynamics along with reorganization of water molecules to stabilize the excess electron.

Ab initio calculations for $X^-(H_2O)_n$ (X = F/Cl/Br/I)[18] as well as $e^-(H_2O)_n$[24] have been extensively studied to determine the minimum energy structures, ionization potentials (IPs), OH stretching frequencies, and CTTS energies. All these small clusters have surface or near-surface bound states. To date, a few models which are contradictory to each other have been proposed to explain the mechanism of photoexcitation of $X^-(H_2O)_n$.[1,25] Therefore, accurate excited-state molecular dynamics (MD) studies have been called upon. However, such studies have hardly been carried out because of either unreliable intermolecular potential parameters or extremely heavy computing resources. Timerghazin and Peslherbe[26] carried out AIMD simulations for an excited-state of $I^-(H_2O)_3$. Kołaski et al.[27] compared AIMD simulations of excited states of $I^-(H_2O)_3$ and $Cl^-(H_2O)_3$ clusters. Cl and I atoms exhibit similar behaviors, whereas their dynamics are slightly different in the time scale. However, there has been a long-standing controversial issue[1,25−27] and yet no clear understanding of the difference in dynamics as the water cluster size of hydrated iodides increases. Here, we investigate the difference in the photoexcitation dynamics between $I^-(H_2O)_{n=2-4}$ and $I^-(H_2O)_{n=5}$ using excited-state AIMD (ES-AIMD) simulations.

2. Calculation Methods

In this work, O and H atoms are treated with the aug-cc-pVDZ+(2s2p/2s) basis set, where the extra diffuse 2s2p and 2s functions are added to all oxygen and hydrogen atoms in order to properly describe the excess electron.[24] In the case of $I^-(H_2O)_n$, large-sized basis sets are necessary to study the excited states, and highly diffuse functions are needed for the study of the dissociation of the anionic species including $e^-(H_2O)_n$. Otherwise, the excess electron of the diffuse nature could be treated as if it were a pseudovalence electron, against the reality. The dependency of basis set on stabilities and electronic properties of iodide−water clusters was investigated in terms of the extra diffuse basis functions and the polarization functions of d-orbitals of oxygen atoms and p-orbitals of hydrogen atoms. The CASSCF(6,6)/aug-cc-pVDZ+X(3s3p/3s) calculations were performed for the $I^-(H_2O)_3$ cluster. The X(3s3p/3s) basis set (the exponents of which are 0.01, 0.00125 and 0.000015625) was used to evaluate the extra basis set for the relative stabilities and vertical detachment energies. We noticed that aug-cc-pVDZ+(2s2p/2s) is reliable for the present study. Since the aug-cc-pVDZ basis set is not available for iodine, the CRENBL effective core pseudopotential (ECP) basis set was used.[28] Calculations were carried out by using the HONDO suite of programs.[29] CASSCF ES-AIMD simulations were performed for the excited states of $I^-(H_2O)_{n=2-5}$ complexes. For clusters comprising up to three water molecules, the active space comprising six electrons and six active orbitals was used [CAS(6,6)]. Because ES-AIMD simulations require enormous computing time for four and five water molecules, the optimal choice of the active space for the reduction of computational resources is needed, even though the computational accuracy is slightly sacrificed. Thus, a reduced active space was used for the practical study of larger complexes on the basis of the following assumptions: (i) We performed CASSCF ES-AIMD simulations for the $I^-(H_2O)_3$ complex using different active spaces [CAS(4,3), CAS(4,4), CAS(6,6)]. The results of these simulations are almost identical; (ii) The excited states

(13) (a) Kloepfer, J. A.; Vilchiz, V. H.; Lenchenkov, V. A.; Germaine, A. C.; Bradforth, S. E. *J. Chem. Phys.* **2000**, *113*, 6288.(b) Choi, J.-H.; Kuwata, K. T.; Cao, Y.-B.; Okumura, M. *J. Phys. Chem. A* **1998**, *102*, 503.
(14) (a) Ayotte, P.; Weddle, G. H.; Kim, J.; Kelley, J.; Johnson, M. A. *J. Phys. Chem. A* **1999**, *103*, 443.(b) Ayotte, P.; Weddle, G. H.; Kim, J.; Johnson, M. A. *Chem. Phys.* **1998**, 239, 485.
(15) Roeselova, M.; Mucha, M.; Schmidt, B.; Jungwirth, P. *J. Phys. Chem. A* **2002**, *106*, 12229.
(16) (a) Thompson, W. H.; Hynes, J. T. *J. Am. Chem. Soc.* **2000**, *122*, 6278. (b) Cabarcos, O. M.; Weinheimer, C. J.; Lisy, J. M.; Xantheas, S. S. *J. Chem. Phys.* **1999**, *110*, 5.
(17) (a) Borgis, D.; Staib, A. J. *Chem. Phys.* **1996**, *104*, 4776. (b) Chaudhury, P.; Saha, R.; Bhattacharyya, S. P. *Chem. Phys.* **2001**, *270*, 277. (c) Roszak, S.; Kowal, M.; Góra, R. W.; Leszczyński, J. *J. Chem. Phys.* **2001**, *115*, 3469.
(18) (a) Majumdar, D.; Kim, J.; Kim, K. S. *J. Chem. Phys.* **2000**, *112*, 101. (b) Kim, J.; Lee, H. M.; Suh, S. B.; Majumdar, D.; Kim, K. S. *J. Chem. Phys.* **2000**, *113*, 5259. (c) Lee, H. M.; Kim, K. S. *J. Chem. Phys.* **2001**, *114*, 4461.
(19) (a) Davis, A. V.; Zanni, M. T.; Weinkauf, R.; Neumark, D. M. *Chem. Phys. Lett.* **2002**, *353*, 455. (b) Kammrath, A.; Verlet, J. R. R.; Bragg, A. E.; Griffin, G. B.; Neumark, D. M. *J. Phys Chem. A.* **2005**, *109*, 11475. (c) Verlet, J. R.; Kammrath, A.; Griffin, G. B.; Neumark, D. M. *J. Chem. Phys.* **2005**, *123*, 231102.
(20) (a) Verlet, J. R. R.; Bragg, A. E.; Kammrath, A.; Cheshnovsky, O.; Neumark, D. M. *Science* **2005**, *307*, 93. (b) Paik, D. H.; Lee, I. R.; Yang, D. S.; Baskin, J. S.; Zewail, A. H. *Science* **2004**, *306*, 672. (c) Hammer, N. I.; Shin, J.-W.; Headrick, J. M.; Diken, E. G.; Roscioli, J. R.; Weddle, G. H.; Johnson, M. A. *Science* **2004**, *306*, 675.
(21) (a) Kim, J.; Lee, J. Y.; Oh, K. S.; Park, J. M.; Lee, S.; Kim, K. S. *Phys. Rev. A.* **1999**, *59*, R930. (b) Kim, J.; Suh, S. B.; Kim, K. S. *J. Chem. Phys.* **1999**, *111*, 10077. (c) Suh, S. B.; Lee, H. M.; Kim, J.; Lee, J. Y.; Kim, K. S. *J. Chem. Phys.* **2000**, *113*, 5273.
(22) Ayotte, P.; Weddle, G. H.; Kim, J.; Johnson, M. A. *Chem. Phys.* **1998**, *239*, 485.
(23) Serxner, D.; Dessent, C. E.; Johnson, M. A. *J. Chem. Phys.* **1996**, *105*, 7231.
(24) (a) Lee, H. M.; Lee, S.; Kim, K. S. *J. Chem. Phys.* **2003**, *119*, 187. (b) Lee, H. M.; Suh, S. B.; Tarakeshwar, P.; Kim, K. S. *J. Chem. Phys.* **2005**, *122*, 044309.
(25) (a) Vila, F. D.; Jordan, K. D. *J. Phys. Chem. A* **2002**, *106*, 1391. (b) Wang, F.; Jordan, K. D. *Annu. Rev. Phys. Chem.* **2003**, *54*, 367. (c) Lee, H. M.; Suh, S. B.; Kim, K. S. *J. Chem. Phys.* **2003**, *119*, 7685. (d) Chen, H.-Y.; Sheu, W.-S. *J. Am. Chem. Soc.* **2000**, *122*, 7534. (e) Chen, H.-Y.; Sheu, W.-S. *Chem. Phys. Lett.* **2001**, *335*, 475. (f) Chen, H.-Y.; Sheu, W.-S. *Chem. Phys. Lett.* **2002**, *353*, 459. (g) Takayanagi, T.; Takahashi, K. *Chem. Phys. Lett.* **2006**, *431*, 28.
(26) Timerghazin, Q. K.; Peslherbe, G. H. *J. Am. Chem. Soc.* **2003**, *125*, 9904.
(27) Kołaski, M.; Lee, H. M.; Pak, C.; Dupuis, M.; Kim, K. S. *J. Phys. Chem. A* **2005**, *109*, 9419.
(28) Basis sets were obtained from the Extensible Computational Chemistry Environment Basis Set Database, developed and distributed by the Molecular Science Computing Facility, Environmental and Molecular Sciences Laboratory, Pacific Northwest Laboratory, P.O. Box 999, Richland, WA 99352 (http://www.emsl.pnl.gov).
(29) Dupuis, M.; Marquez, A.; Davidson, E. R. HONDO 99.6, (1999), based on HONDO 95.3, M. Dupuis, A. Marquez, E. R. Davidson, Quantum Chemistry Program Exchange (QCPE), Indiana University, Bloomington, IN 47405.

or charge-transfer states of the $I^-(H_2O)_n$ complex [relevant to the transition between the highest occupied molecular orbital (HOMO) and the lowest unoccupied molecular orbital (LUMO)] arise from the excitation of the electron localized on the iodide anion to a more delocalized state on the water cluster. Since the promotion energies are larger than the electron affinities for the iodine atom, and the iodine's p-orbital pointing toward the water cluster is different from that of the other two p orbitals, the active space of CAS(4,4) contains the essential MOs involved in the photoexcitation and the rearrangement of the water cluster including the excess electron. In this regard, for the reliable understanding of the dissociation phenomena of $I^-(H_2O)_{n=4,5}$, CAS-(4,4) is the only feasible and yet the most up-to-date approach currently available.

The ES-AIMD simulations of the $I^-(H_2O)_{n=2-5}$ clusters were carried out for 800 fs ($n = 2-4$) and 600 fs ($n = 5$) with a time step of 0.2 fs. Shorter time scale simulations for $n = 5$ (300 fs) were also carried out with a time step of 0.1 fs. The initial structures having the ground-state minimum-energy geometry of $I^-(H_2O)_{n=2-5}$ (optimized at the CASSCF/aug-cc-pVDZ+(2s2p/2s) level) were vertically excited. In addition, somewhat different initial geometries and different initial kinetic energies (*KE*) were also studied in consideration that they could significantly affect the conformational changes during the simulations. We set the initial *KE* (KE_0) of the ground-state $I^-(H_2O)_{n=2-5}$ clusters to 0 and 300 K. In particular, in the case of $I^-(H_2O)_5$ which shows complex dynamics behavior, we studied the cases with the KE_0 of 0, 100, 200, 300, and 400 K, and furthermore, additional cases with different initial velocities at 300 and 400 K, and another case with different initial geometry at 300 K. The individual starting velocities at finite temperatures were assigned according to the classical Boltzmann distribution.[30] Since there is no significant difference between the two temperatures, many different simulations with different initial velocities may not be needed. Thus, we report only the case of 0 K.

For the simulations, one may consider the NVE ensemble. However, in this case, the excitation energy of $I^-(H_2O)_{n=2-5}$ (4.0−4.5 eV)[23] is much higher (by 0.5−1 eV) than the sum of the electron affinity of the iodine (3.06 eV)[31] and the iodine−water binding energy (∼0.5 eV).[18] Then, as time elapses, the *KE* becomes so high (≳500 K) that each cluster tends to be almost fully dissociated into the iodine radical, water monomers, and an excess electron. Namely, the average kinetic energy per water molecule is ∼5 kcal/mol, which should be compared with the free binding energy of the water dimer which is ∼0 kcal/mol at 230 K and ∼3 kcal/mol at 0 K (Even the zero-point energy uncorrected binding energy at 0 K is ∼5 kcal/mol).[32] Then, while hot clusters are almost fully dissociated, only colder clusters would retain the original water cluster size without dissociation into smaller clusters. Therefore, as time elapses, the NVE ensemble would change into the NVT-like ensemble. In this regard, we considered slow damping for the *KE* in simulations Then, in the initial stage, the system behaves like the NVE ensemble, but as time evolves, the temperature of clusters decreases. This would be similar to the experimental situation that the temperature of clusters eventually quenches to that of heat bath.

At the CASSCF level the dynamical correlation effects are not taken into account; thus, the dispersion energy cannot be properly recovered at this level of calculations. The dispersion energy is important for dipole-bound electrons.[24] Therefore, AIMD simulations based on the complete active-space second-order perturbation theory (CASPT2) method seem to be more reliable. However, we should understand that CASPT2 is computationally very demanding and in many cases diverges due to the "intruder state" problem. We performed single-point CASPT2 calculations for selected geometries for $I^-(H_2O)_{n=2-5}$ clusters. The second-order perturbative correction significantly decreases the total electronic energy, but the differences between CASPT2 and CASSCF energies are almost constant (Figure 1). Thus, the energy change in the CASSCF approach is similar to that in the CASPT2 approach, because the dispersion energies of the same-sized clusters are almost equivalent.

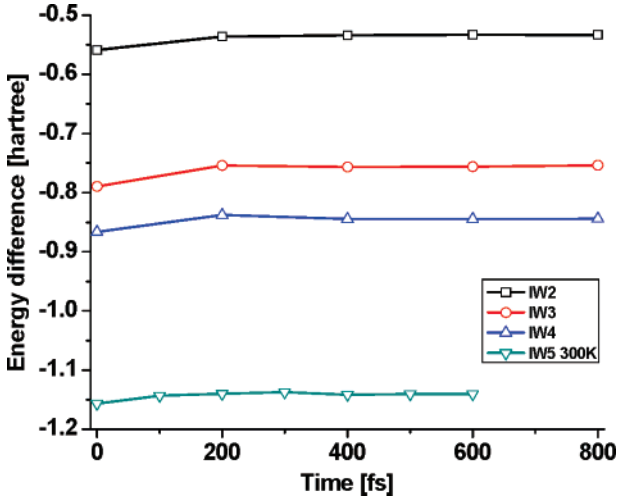

Figure 1. Difference between CASPT2 and CASSCF energies [hartree] for $I^-(H_2O)_{n=2-5}$ clusters.

Table 1. CTTS Energies (eV) of $I^-(H_2O)_{2-5}$[a]

	CIS	TD- DFT	CAS- SCF	CAS- PT2	SAC- CISD	expt[b]
$I^-(H_2O)_2$	5.07	3.53	4.36	4.26	4.47	3.95
$I^-(H_2O)_3$	5.46	4.16	4.94	4.70	4.82	4.25
$I^-(H_2O)_4$	5.60	4.35	5.11	4.86	4.93	4.50
$I^-(H_2O)_5$	5.63	4.18	5.02	4.83	4.81	

[a] The basis set used is aug-cc-pVDZ+(2s2p/2s) for O and H and CRENBL ECP for I. Our previous theoretical values using different basis sets are in ref 18. [b] Reference 23.

Many reactions involved in the excited electronic state would be properly described within the adiabatic Born−Oppenheimer approximation. It may, however, be violated when the energy splitting between adiabatic potential energy surfaces is comparable to that of the corresponding non-adiabatic couplings. Although the non-adiabatic effects would not be so significant in the present case, this consideration would be desirable. However, at present it is not possible to incorporate the non-adiabatic couplings in molecular dynamics simulations.

3. Results

Table 1 lists the CTTS energies of $I^-(H_2O)_{2-5}$ calculated at various levels of theory. The CASSCF predicted values are in reasonable agreement with the experimental values.[23]

The ES-AIMD simulations for an excited state of $I^-(H_2O)_{2-4}$ exhibit simple dissociation, while that of $I^-(H_2O)_5$ shows drastic rearrangement. Snapshots of the time evolution of structures and excess electron densities of the $I^-(H_2O)_{n=2-5}$ clusters upon the excitation are drawn in Figures 2 and 3, respectively. The evolutions of *KE*s of the iodide atom and water molecules are depicted in Figure 4. The time evolutions of the iodine−oxygen distances [r(I···O)] and the inter-oxygen distances [r(O···O)] are shown in Figures 5 and 6, and the time evolution of natural bond orbital (NBO) charges[33] of the iodide atom and water

(30) Kim, K. S.; Nguyen, H. L.; Swaminathan, P. K.; Clementi, E. *J. Phys. Chem.* **1985**, *89*, 2870.
(31) Hanstorp, D.; Gustafsson, M. *J. Phys. B: At. Mol. Opt. Phys.* **1992**, *25*, 1773.
(32) (a) Kim, K. S.; Mhin, B. J.; Choi, U-S.; Lee, K. *J. Chem. Phys.* **1992**, *97*, 6649. (b) Mhin, B. J.; Lee, S. J.; Kim, K. S. *Phys. Rev. A* **1993**, *48*, 3764. (c) Lee, H. M.; Suh, S. B.; Lee, J. Y.; Tarakeshwar, P.; Kim, K. S. *J. Chem. Phys.* **2000**, *112*, 9759.
(33) Glendening, E. D.; Badenhoop, J. K.; Reed, A. E.; Carpenter, J. E.; Bohmann, J. A.; Morales, C. M.; Weinhold, F. NBO 5.0 program (2001), Theoretical Chemistry Institute, University of Wisconsin, Madison.

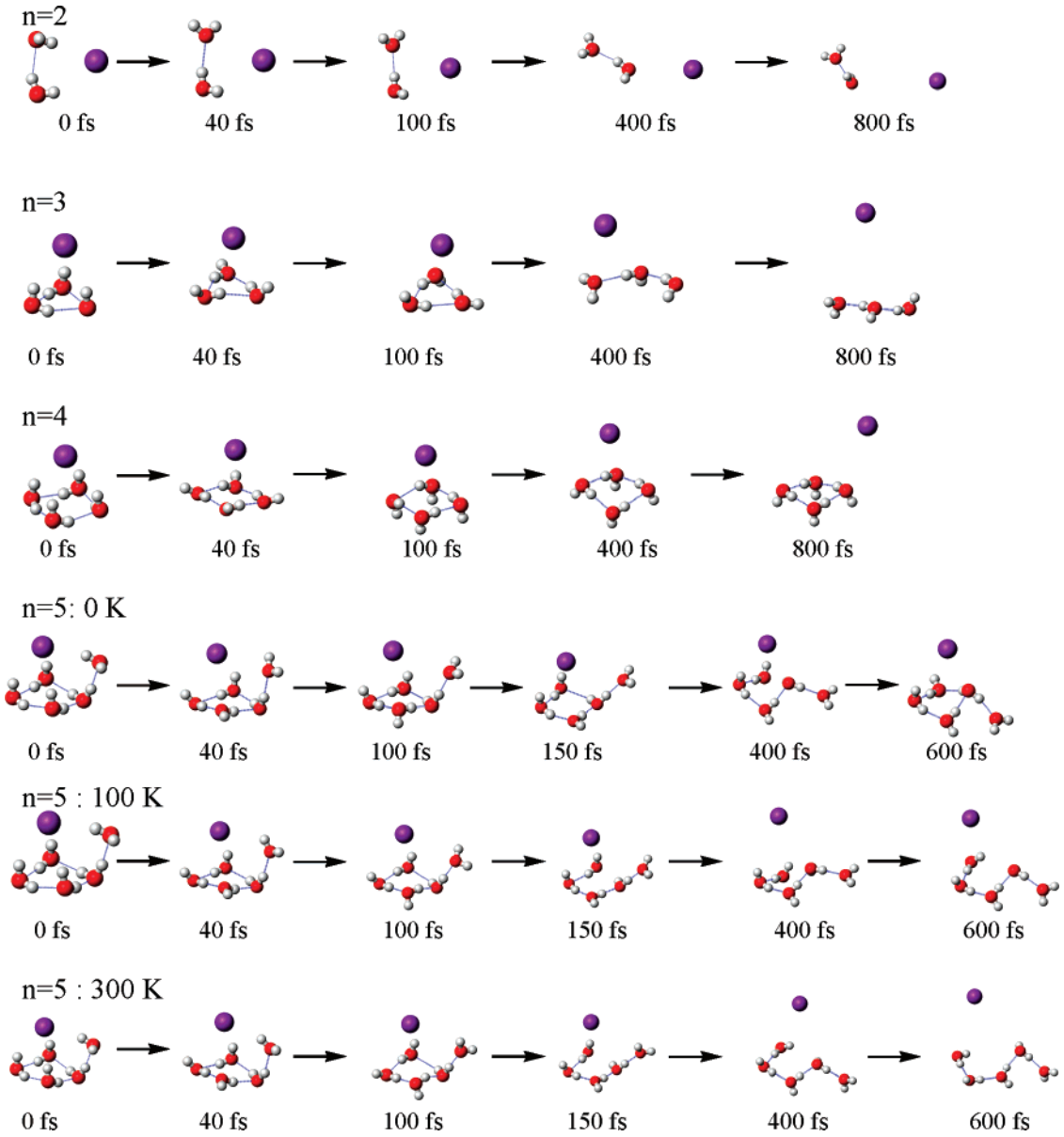

Figure 2. Snapshots of the evolving process of $I^-(H_2O)_{n=2-5}$ clusters upon excitation taken from excited-state ab initio molecular dynamics simulations. All the cases are for KE_0=0 K except for cases $n = 5$ which are for $KE_0 = 0$, 100 and 300 K.

molecules is depicted in Figure 7. The time evolution of the total potential energy of the cluster is shown in Figure 8.

For $I^-(H_2O)_{n=2-4}$, the simulation results for $KE_0 = 300$ K (not shown here) are overall similar to those of 0 K. This is partly because the *KE* of one H atom (or H atoms), which is in close contact with the iodide, increases drastically up to ~1000 K (or several kcal/mol) within the first ~30 fs of the simulation (Figure 4). Thus, the additional kinetic energy due to the initial kinetic energy of a few hundred K does not significantly affect the overall dynamics of the clusters. Since the simulations with the initial zero *KE* (i.e., $KE_0 = 0$ K) are unique and furthermore very similar to the representative one (due to the most probable distribution) among many samplings at low temperatures, we here discuss only the cases of $KE_0 = 0$ K for $I^-(H_2O)_{n=2-4}$. In the case of $I^-(H_2O)_5$ which shows complex dynamics, we performed a number of ES-AIMD simulations with different KE_0's (0−400 K), different sets of velocities, different initial geometries, and different time steps. No important differences between simulation results were noted at the same temperature. However, there appear apparent differences in the final structures between different temperature simulation results ($n = 5$ in Figure 2).

Upon the excitation, $I^-(H_2O)_n$ releases the iodine radical, resulting in the formation of the water clusters containing the excess electron $[e^-(H_2O)_n]$. Their time evolutions are as follows. Before the excitation, the iodide anion interacts with the positively charged H atoms of water molecules with almost ionic interaction at a short H-bond distance. Upon the excitation (at 0 fs), the electron density changes instantly from the iodide to the water cluster (Figure 3), and then the strong ionic $I^-\cdots H^{\delta+}$ interactions at a short H-bond distance are instantly replaced by the strong repulsion between the neutralized iodine radical and the H atom(s) of the water clusters ($I^\bullet\cdots H$ repulsion). Thus, the iodine radical begins to release from the water cluster, resulting in the fast increase of *KE* in the H atoms involved in the OH reorientation. In the beginning, the H atoms rotate along the O···O axis away from the iodine radical so that the cluster structure can be reasonably stabilized (Figure 2). Within ~30

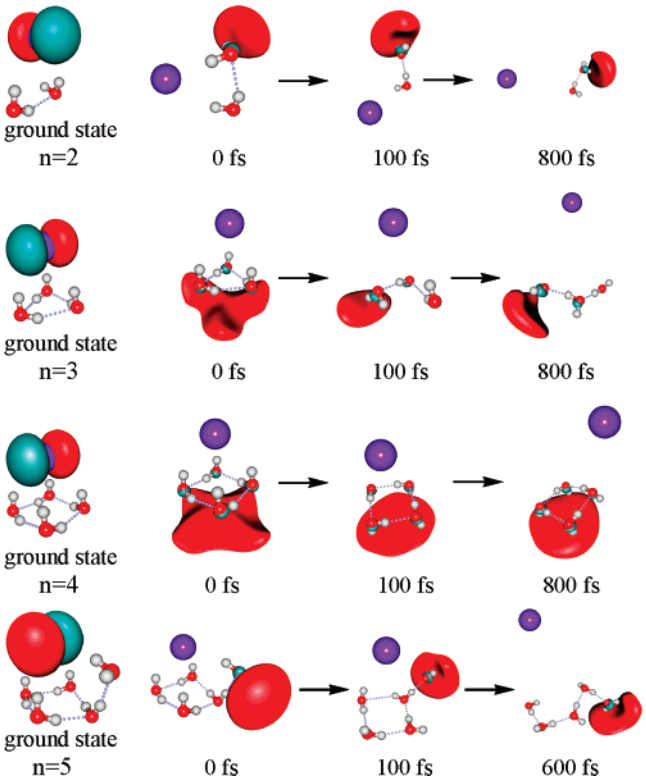

Figure 3. Snapshots of the evolving process of the excess electron density of $I^-(H_2O)_{n=2-5}$ clusters upon excitation. All the cases are for KE_0=0 K except for $n = 5$ which is for $KE_0 = 300$ K.

fs, the *KE* of the H atom attached to O1 (which is nearer to I than O2 is) is maximized (Figure 5), as the I•···H repulsion weakens, while the sudden excessive rotation increases the torsional energy for the rotation of the H atoms through the O···O axis. Then, this excessive rotation helps rearrange the H atoms until ∼60 fs. After ∼60 fs, the O atoms (i.e., the water network) begin to undergo the rearrangement (Figure 6). Around ∼100 fs, the reconstruction of the water network (such as bond opening) is partly done. After ∼100 fs, the reconstruction is slowly made.

If the initial water cluster conformation of the complex is in a less stable or metastable conformational region of $e^-(H_2O)_n$, it would eventually change to the lower-energy conformation. In Figures 2 and 5, as time evolves, the iodine radical releases; while $I^-(H_2O)_2$ gives the structure of $e^-(H_2O)_2$, the $I^-(H_2O)_3$ cluster undergoes a simple ring-opening process from the triangular to linear structure and eventually changes to the linear structure of $e^-(H_2O)_3$, and $I^-(H_2O)_4$ forms the cyclic anionic water tetramer $e^-(H_2O)_4$ whose structure is completely oppositely reoriented with respect to the initial cyclic structure. In the case of $I^-(H_2O)_5$, the structure undergoes a complicated rearrangement process. The energy gain (∼1 eV) upon the excitation is distributed to five water molecules as well as the iodine radical, giving the average energy of ∼4 kcal/mol per water molecule which is slightly larger than the H-bond-breaking energy of the water dimer (∼3 kcal/mol at 0 K) but comparable to that of the water pentamer (∼5 kcal/mol at 0 K and ∼0 kcal/mol at 230 K).[32] Then, as a small amount of KE_0 (e.g., 100 K or ∼1 kcal per water molecule; 200 K or ∼2 kcal/mol per water molecule) is added to the cluster, the conformational transition barriers can be easily overcome. Thus, in this case, the initial temperature effect becomes important. A more detailed description of the simulation results of $I^-(H_2O)_{n=2-5}$ is given below.

$I^-(H_2O)_2$. For the $I^-(H_2O)_2$ cluster, we observe a simple mechanism of the electron transfer from the iodide to the water cluster (Figure 3), followed by the iodine detachment along with the charge redistribution over the water dimer. The analysis of r(I···O) shows that the time evolutions of two water molecules are different (Figure 5). The water molecules form a dimer during the MD simulation since the *KE* is slowly damped as time elapses. Without damping, the cluster would be completely dissociated into the iodine radical, two water monomers, and a free electron. Thus, the electron release would be observed from the hot dissociated clusters. Upon the excitation, at 0 fs, the excess electron density of the iodine instantly transfers to the outer vacant space around the dangling H atom of the water molecule (H_2O-2) (the proton acceptor which can eventually be transformed to the double proton acceptor: AA), though it is less near to the iodine. For the first 30−40 fs, owing to the strong I•···H repulsion for H_2O-1 (against the strong I^-···H interaction on the ground state), the distances between the I• radical and two H atoms increase with acceleration (showing high curvature of the curve for distance vs time, toward the stabilization of the cluster) by changing the orientation of the rapidly moving H atoms about the slowly moving heavy O atoms in the water molecules. In this way, the reduction of I•··H repulsion by reorientations of H atoms stabilizes the cluster, resulting in drastic lowering of the potential energy of the cluster. Thus, the first local minimum along the time evolution of the potential energy occurs at ∼30 fs (Figure 8) with the maximized *KE* (∼5 kcal/mol) of H_2O-1 (Figure 4). After ∼40 fs, the I···O distance [r(I···O)] increases slowly and steadily. The water molecule denoted as H_2O-1 (proton acceptor) close to the iodine atom starts to be repelled much faster than the other water molecule denoted as H_2O-2 (proton donor). After 80 fs, the distance from the oxygen of H_2O-1 to the iodine atom becomes longer than that from the oxygen of H_2O-2 (Figure 5). The O1−O2 distance [r(O1−O2)] oscillates between 2.6 and 3.3 Å, keeping the H-bonding in cold clusters due to the *KE*-damping (Figure 6). Given that the experimental radial distribution function of the liquid water gives the first minimum distinguishing between the first and second hydration shells,[34] the H bond is loosened for the interoxygen distance over 3.4−3.5 Å, and this distance is related to the turning point for the H-bond breaking. Without the *KE*-damping, the H-bond in the water dimer would break, and the excess electron would be released. The period of the O1−O2 stretching vibration mode (Figure 6) is ∼200 fs. The investigation of NBO charges (Figure 7) leads to the prediction that at 0 fs the iodine and H_2O-2 are almost neutral, while H_2O-1 is negatively charged (−0.78 au). After 800 fs, the cold structure of the excess-electron water dimer resembles the most stable 2CsC conformer (though more accurate description should be given as the quantum probabilistic structure),[21] due to the strong electron−dipole (e−μ) interaction.

$I^-(H_2O)_3$. In the case of $I^-(H_2O)_3$, the geometry of the excess-electron water cluster changes significantly from the initial structure. In the beginning, three water molecules form a stable cyclic trimer with three H atoms pointing toward the iodide

(34) (a) Soper, A. K. *Chem. Phys.* **2000**, *258*, 121. (b) Soper, A. K.; Philips, M. G. *Chem. Phys.* **1986**, *107*, 47. (c) Kim, K. S. *Chem. Phys. Lett.* **1989**, *159*, 261. (d) Sharp, K. A.; Madan, B.; Manas, E.; Vanderkooi, J. M. *J. Chem. Phys.* **2001**, *114*, 1791.

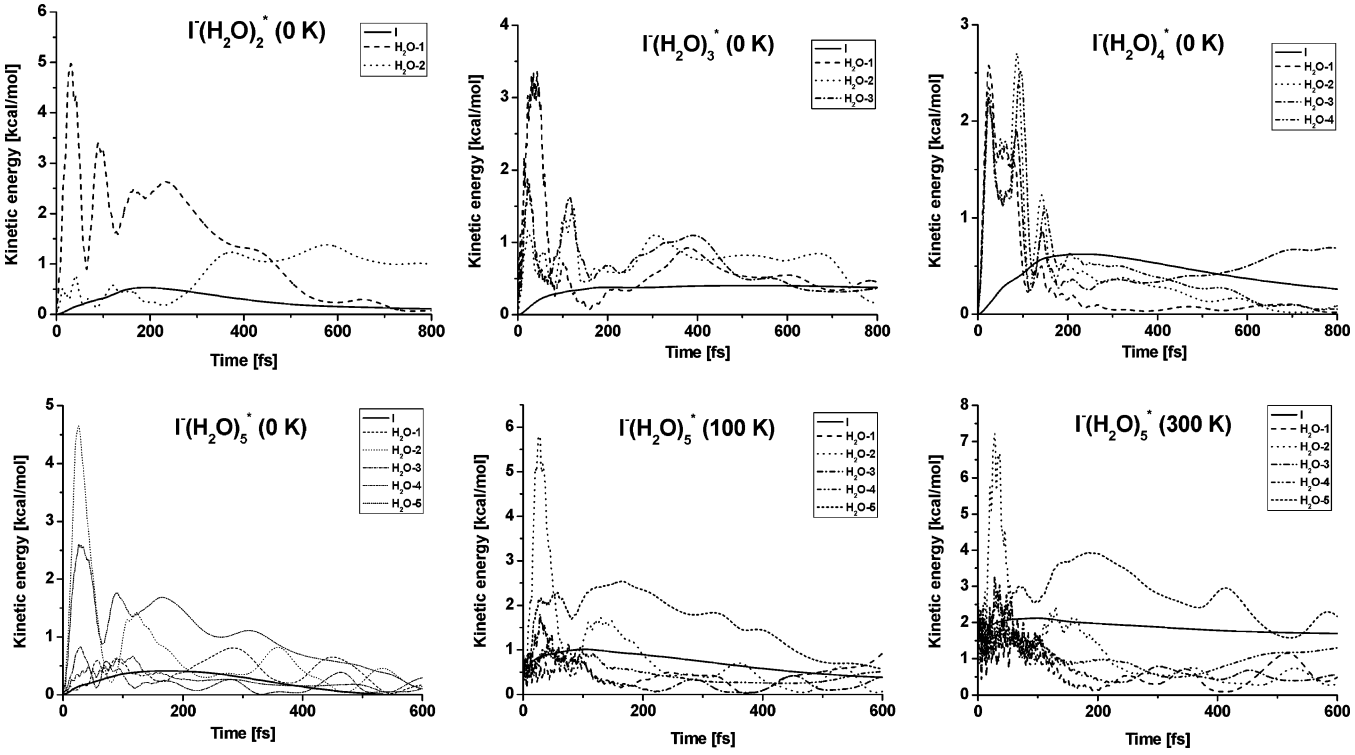

Figure 4. Time evolution of the kinetic energy of the iodide atom and water molecules of $I^-(H_2O)_{n=2-5}$ clusters. The value (in K) in parentheses denotes KE_0.

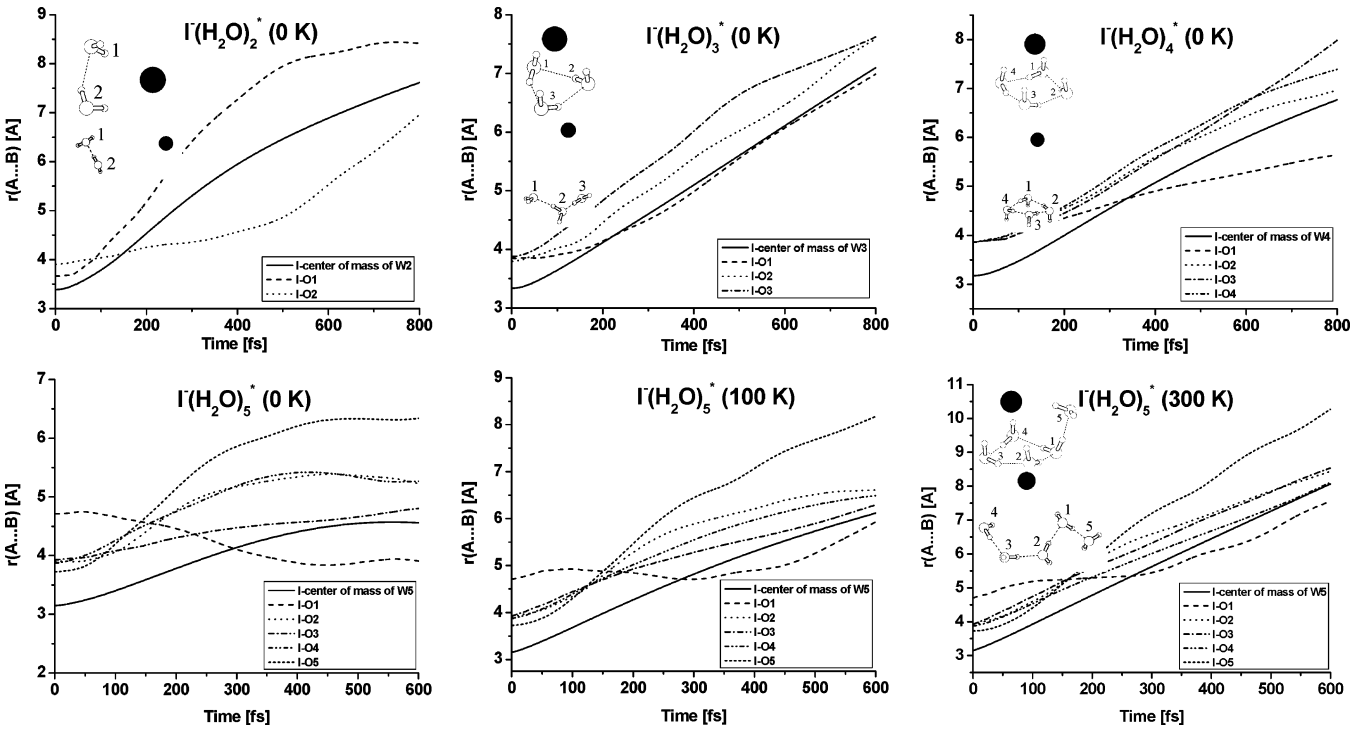

Figure 5. Time evolution of r(I···O) distances (in Å) for $I^-(H_2O)_{n=2-5}$ clusters. Two molecular structures drawn in insets in each figure denote the initial geometry (upper inset) and the final geometry at the end of the simulation (lower inset).

anion. Upon the excitation, at 0 fs, the excess electron density of the iodide instantly transfers to the opposite side of the triangular plane of the water trimer. For the first ∼40 fs, owing to the strong I•···H repulsion, the distances between the I• radical and three H atoms increase rapidly by changing the orientation of the rapidly moving H atoms about the slowly moving heavy O atoms in the water molecules (Figure 2). Thus, the r(I···O) increases slowly in the beginning (Figure 5). After ∼100 fs, the water molecules begin to rearrange themselves because during the H reorientation the three I•···H distances are somewhat different from each other, and one of H-bonds weakens more or is partly broken due to the significantly bent angle of OH···O. This results in the emergence of the AA-type dangling H atoms which enhances the dipole moment, and so

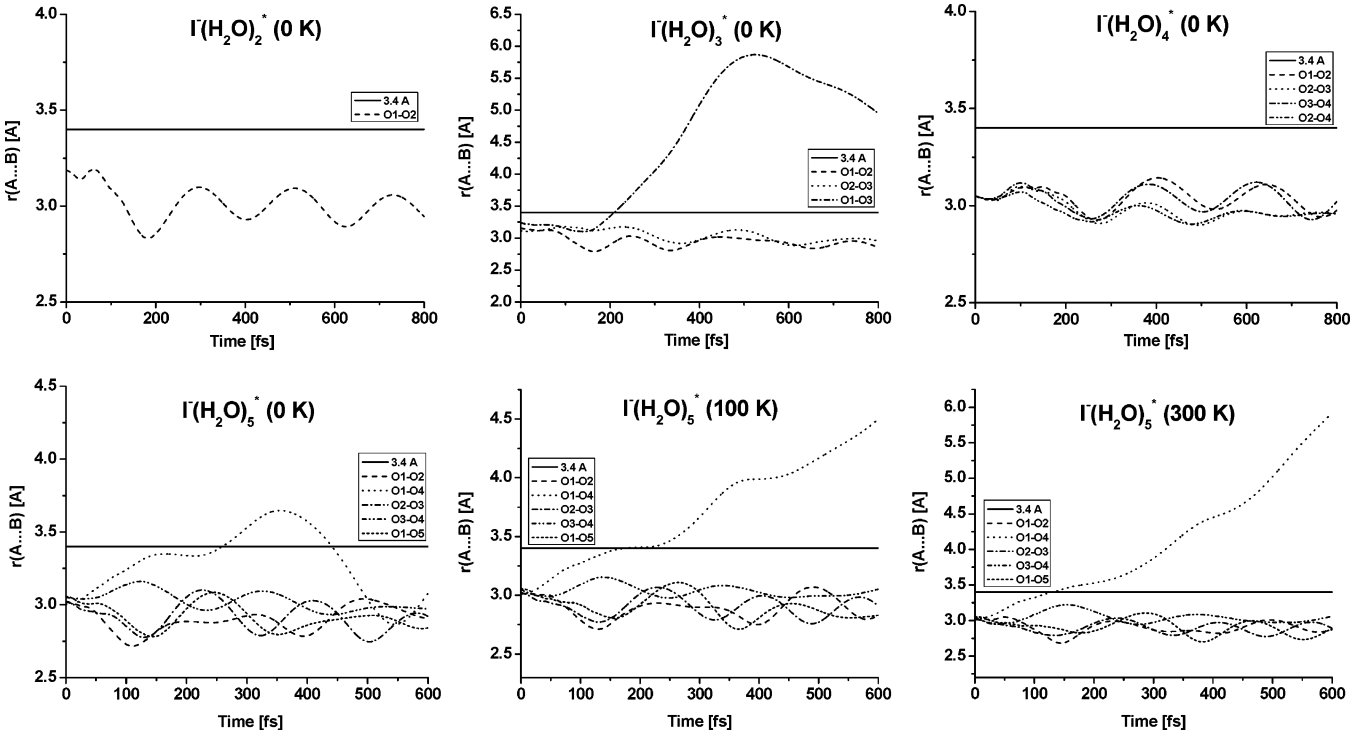

Figure 6. Time-evolution of r(O···O) distances for $I^-(H_2O)_{n=2-5}$ clusters.

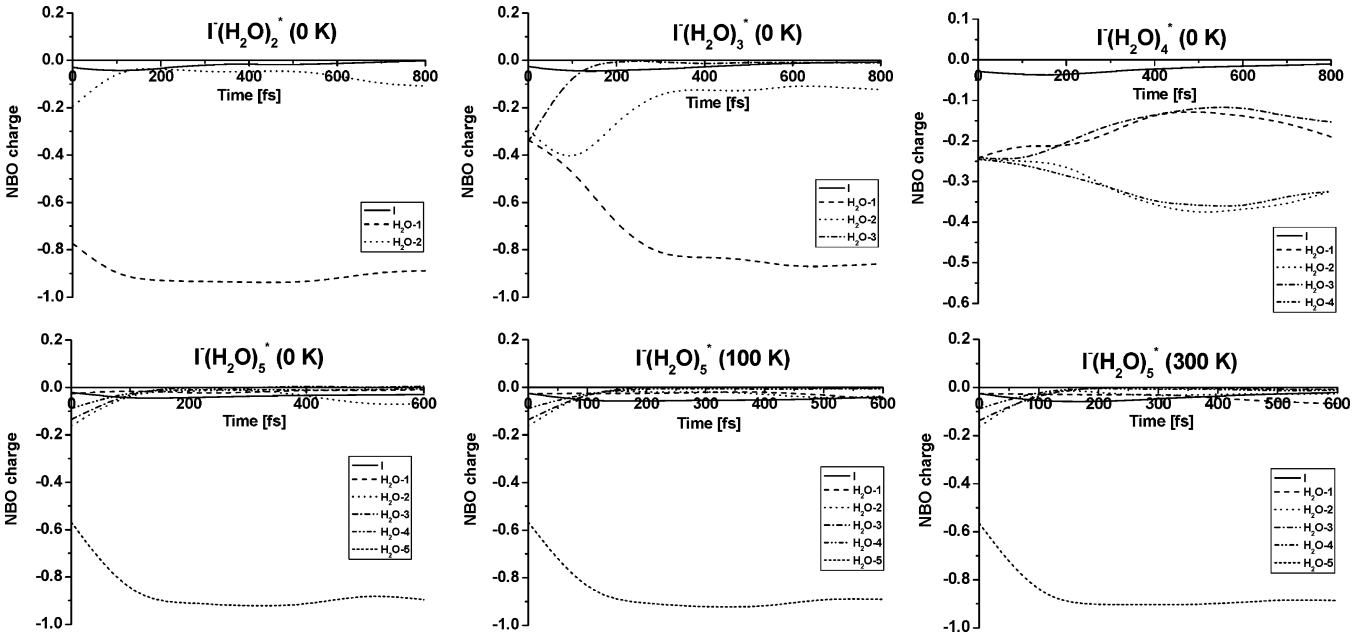

Figure 7. Time evolution of NBO charges localized on the iodine atom and water molecules.

the three O···O distances begin to be different to form a more stable linear structure of $e^-(H_2O)_3$. After 200 fs, the cyclic trimer is completely open (the O1−O3 distance is 3.4 Å). As time elapses, this inter-oxygen distance continuously increases. At 500 fs, it reaches the maximum value (5.6 Å) which is a fully extended linear water chain, while after that the distance shows oscillations. The bending/linear oscillations show the period of ∼250 fs.

As for the charge distribution, in the beginning, the negative charge is evenly distributed over the whole water cyclic trimer. During 200 fs, the charge is quickly redistributed, and one water molecule (AA type) becomes negatively charged due to the surrounding excess electron density, while the other two become almost neutral. Thus, the dipole moment of the water cluster (excluding the excess electron) increases.

In the case of the excess-electron water trimer, the cyclic ring structure is the most stable, but it has negligible VDE (0.00−0.01 eV).[21] Then, the rapid tunneling effect is expected to make no distinction between the cyclic excess-electron water trimer (i.e., the system that a nearly free electron is bound to the neutral water trimer) and the system composed of the neutral cyclic water trimer and a free excess electron. Therefore, the lowest-energy structure for the electron water trimer is considered to be the linear conformer with the VDE of 0.13 eV, in agreement

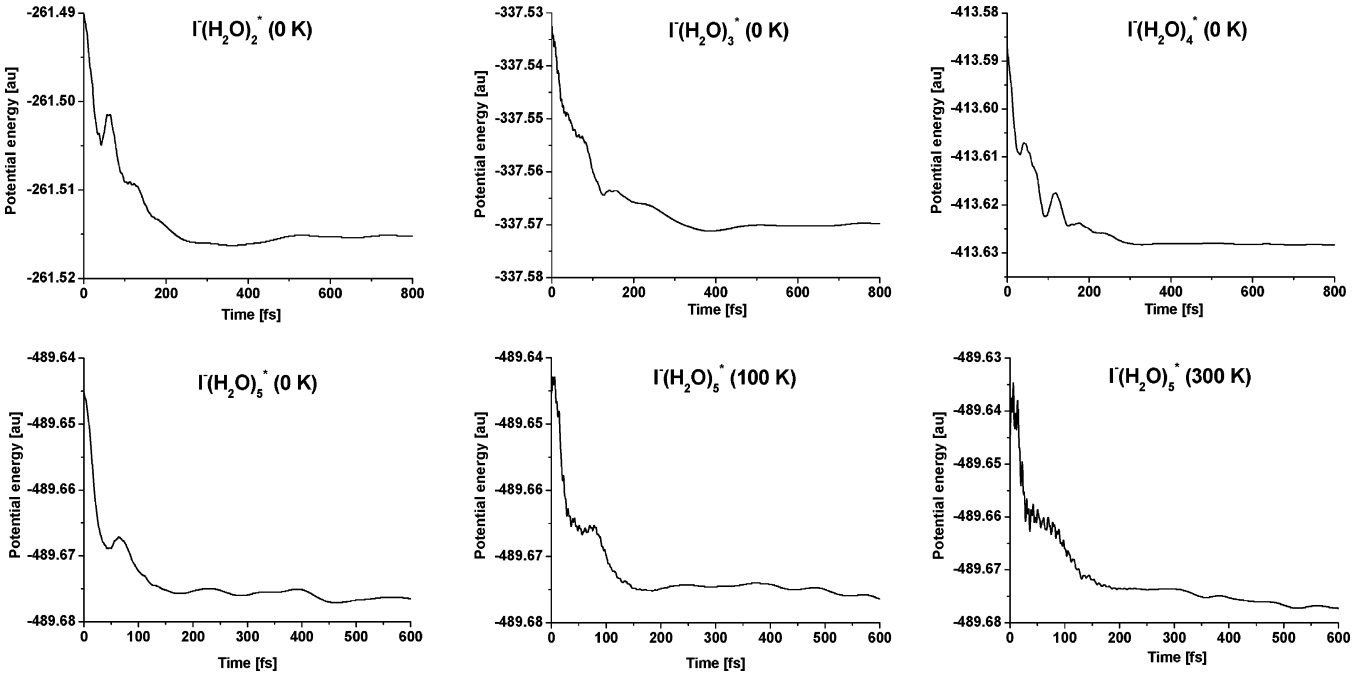

Figure 8. Time evolution of the potential energy of the $I^-(H_2O)_{n=2-5}$ clusters.

with the experimental value (0.13 eV).[24] The *KE* of the neutral iodine is almost constant during simulation (<0.5 kcal/mol). The *KE* of water molecules increases in the beginning (for 50 fs) due to the I···H repulsion upon the excitation, which results in reorganization of the water network. During simulations, the *KE* of water molecules fluctuates (Figure 4). The I•···H repulsion (instead of the I•···O repulsion) takes place in a short time scale of dynamics, and this eventually leads to the rearrangement process of the O atoms toward the linear excess-electron water cluster.[24]

$I^-(H_2O)_4$. For $I^-(H_2O)_4$, the topology of the cyclic water tetramer is conserved during the simulation. In the beginning, the water tetramer forms a planar cyclic ring with H atoms pointing toward the iodide. Upon the excitation, at 0 fs, just like the case of $I^-(H_2O)_3$, the excess electron density of the iodide instantly transfers to the opposite side of the tetragonal plane of the water tetramer. For the first ~40 fs, the distances between the I• radical and three H atoms increase rapidly by changing the orientation of the rapidly moving H atoms due to the strong I•···H repulsion (Figure 2). Thus, the *r*(I···O) increases slowly, and so after 100 fs, water molecules comprising the water network are completely reoriented with respect to the initial geometry. The analysis of inter-oxygen distances shows that they do not change significantly during the MD simulation. Thus, the overall rearrangement of the water cluster during the MD simulation is minimal. Upon the excitation, the negative charge transferred from the anionic precursor to the water tetramer is evenly distributed over the water tetramer network. The charge redistribution during the simulation is not significant because the tetramer ring structure is conserved during the simulation, while the charges localized on water molecules fluctuate (Figure 7), since the excess electron is delocalized inside the tetragonal ring structure. During the first ~30 fs the *KE* of each water molecule increases up to 2.5 kcal/mol due to the rapid rotation of water molecules (i.e., H reorientations) (Figure 4). The total potential energy evolution indicates that the excess-electron water tetramer (which is the global minimum) is formed around 90 fs (Figure 8).

$I^-(H_2O)_5$. In the ground state, the water pentamer cluster in $I^-(H_2O)_5$ has a planar cyclic water tetramer with a water molecule attached to the tetramer through a H-bond. For the $I^-(H_2O)_5$ complex, we performed (i) five different ES-AIMD simulations of $KE_0 = 0$, 100, 200, 300, and 400 K, (ii) two additional different ES-AIMD simulations of $KE_0 = 300$ and 400 K (with different initial velocities and smaller time steps of 0.01 fs) using the initial geometry of the CASSCF/aug-cc-pVDZ+(2s2p/2s) ground-state minimum-energy geometry, and (iii) two extra ES-AIMD simulations of $KE_0 = 0$ and 300 K using different initial geometries (not the minimum energy geometry). The simulation results are overall similar, but there is a significant difference in structures and electronic properties (dipole moment, VDE) between the 0 K and 100−400 K simulations (Figure 2). The latter has the linear-like structure due to the entropy effect (which tends to have more flexible structures with fewer H-bonds), while the former has a tetragonal ring because the final structure for $KE_0 = 0$ K is more stabilized by an additional H-bond than the linear structures for $KE_0 =$ 100−400 K. However, the skeletons for $KE_0 = 0$ K and 100−400 K are similar except that the former has one additional H-bond near the quasi-tetragonal ring shape of the linear structure. In this regard, except for $KE_0 = 0$ K, all the results are overall similar regardless of the initial geometry and different velocities. We find that this is due to the fact that above ~100 K the linear structure of $e^-(H_2O)_5$ is more stable in free energy than the tetragonal ring structure. As compared with the tetragonal ring structure, the linear structure is 1.0 kcal/mol less stable at 0 K, but begins to be more stable above 100 K and 4.2 kcal/mol more stable at 298 K at the B3LYP/6-311++G**-(sp) level of theory. We discuss two representative simulation results for $KE_0 = 0$ and 300 K.

For the KE_0 of 0 K, the topology of the cyclic water tetramer is conserved during the simulation; however, the hydrogen bond

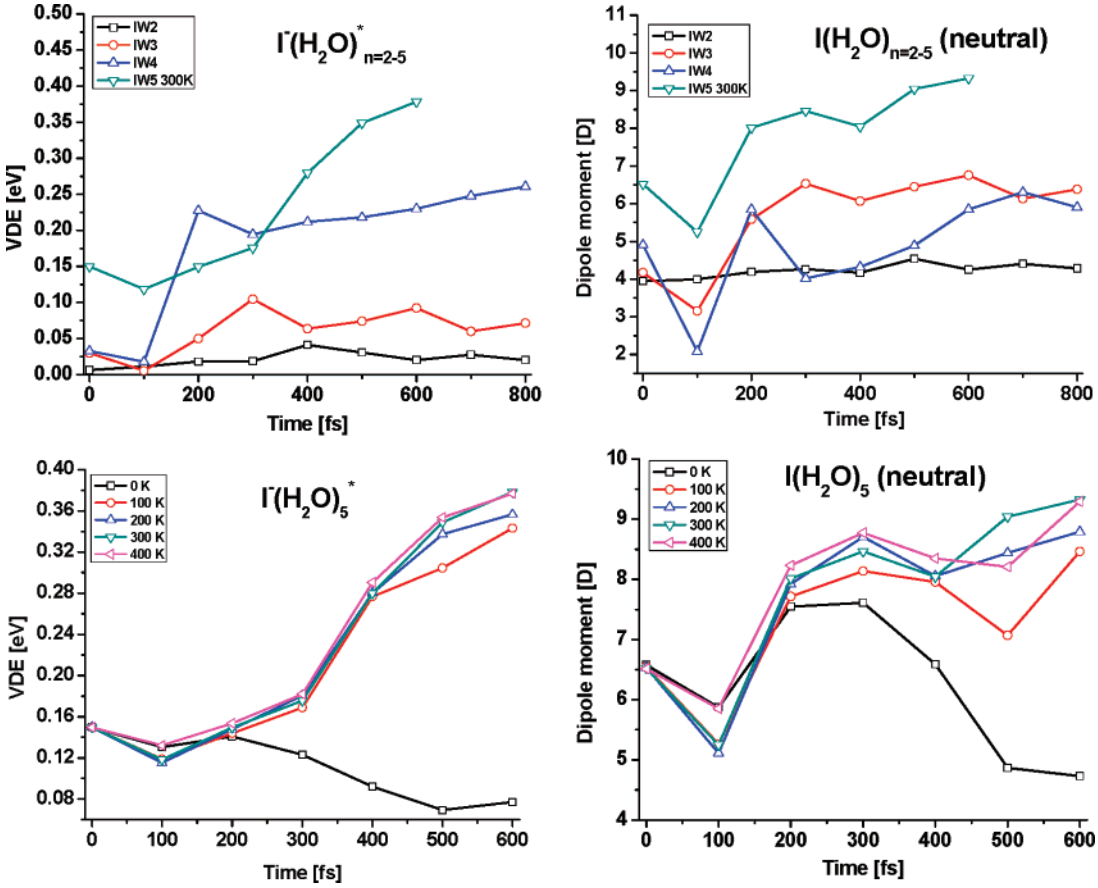

Figure 9. Time evolution of the vertical detachment energy (VDE) for $I^-(H_2O)_{n=2-5}$ and the dipole moment of the neutral state on the $I^-(H_2O)_{n=2-5}$ geometries. For $I^-(H_2O)_5$ time evolutions of VDE are drawn for different initial temperatures.

between H_2O-1 and H_2O-4 is broken for a while (for ~300 fs). For the KE_0 of 100−400 K, the cyclic water tetramer is converted to a quasi-linear chain. These final structures reflect the entropy-driven dynamics. Although the structural evolution for the KE_0 of 0 K does not reproduce the experimental VDE evolution, those for the KE_0 of 100−400 K are in excellent agreement with the experiment. This implies that the temperature in the experiment would be 100−400 K. When the initial temperature increases, the cyclic water tetramer opens faster. At higher temperatures, the iodine radical releases faster from the system. Additional simulations for $KE_0 = 300$ and 400 K using different initial velocities indicate that the effect due to the different initial velocities is not significant.

From the charge analysis, the dangling water molecule (proton acceptor) has half the total negative charge at 0 fs and nearly the total negative charge after 100 fs, whereas the other water molecules are almost neutral. The potential energies of the clusters tend to decrease with the evolution of time (Figure 8). During the simulation, the excess electron-water cluster changes significantly with respect to the initial structure. The planar cyclic tetramer with the dangling water molecule is converted to a quasi-linear chain. As shown in Figure 2, the fast moving H atoms move away from the iodine radical through the reorientation along the O atoms of the water molecules, and are out of the repulsion region in 20−30 fs. The reorientations of H atoms continue to form a more stable conformation in terms of the H reorientation till 50 fs. After 50 fs, the slowly moving O atoms (i.e., the water network) begin to undergo the rearrangement to form a more stable conformer. Around ~120 fs, the drastic reconstruction of the water network (such as bond opening) is partly done. After ~120 fs, the reconstruction is slowly made. In the beginning of the simulation, the *KE*s of H_2O-2 and H_2O-5 are remarkably larger (Figure 4) than for other water molecules. However, the increased *KE*, though damped, is not small, and the resulting excess-electron water cluster tends to have the minimum free energy structure.

Vertical Detachment Energy. For the $I^-(H_2O)_5$ cluster, we computed VDEs for the different conformations formed during ES-AIMD simulations of $KE_0 = 0$, 100, 200, 300, and 400 K using the CASSCF ground-state minimum energy geometry (Figure 9). Accurate calculation of VDEs for the excited state of anion−water clusters is a challenging problem for electronic structure calculations because the dispersion forces contribute significantly to the electron binding. The VDE evolution of the excited state of halide−water cluster was thus calculated by using our previous approach.[24] The experimental VDEs of $I^-(H_2O)_n$* are estimated to be 0.03, 0.08, and 0.16 eV for clusters $n = 2$, 3, and 4, respectively.[24] For the VDE of $I^-(H_2O)_5$*, the shift from 0.15 to 0.4 eV was observed in the experiment around 600 fs after the excitation.[19] This is demonstrated from the calculated VDEs which increase from 0.15 to 0.38 eV during 600 fs. This demonstrates that the cluster for $n = 5$ involves complex dynamics with significant reorganization of the water network to more effectively stabilize the excess electron against the simple population decay of the cluster for $n = 2-4$. Although the changes in VDE calculated at different temperatures are not

identical, the abnormal shift in VDE is observed for the case of KE_0 above 100 K.

We calculated dipole moments of neutral $I(H_2O)_{n=2-5}$ complexes (Figure 9). It is evident that the VDE is strongly correlated with the dipole moment of the corresponding neutral $I(H_2O)_{n=2-5}$. The VDE is dominated by the electron−dipole interactions. In the case of $I^-(H_2O)_5$ clusters with $KE_0 = 100-400$ K, the water network is reorganized to increase the dipole moment. The increase in dipole moment is strongly correlated with the emergence of the double proton acceptor (AA) of the dangling water molecule in the cluster. This dynamics-driven molecular rearrangement process tends to lead to the formation of the entropy-driven linear structures because of the increased kinetic energy.

Discussion

In the beginning of ES-AIMD simulations of $I^-(H_2O)_n$, the *KE* rapidly increases due to the strong repulsion between the iodine atom and the H atoms in the water cluster. Thus, the H atoms reorient very fast, resulting in the fast release of the iodine radical. On the other hand, the slowly moving O atoms begin to affect the reorganization of the excess-electron water network at ∼50 fs. Therefore, except for the initial strong I•···H repulsion at the initial stage upon the excitation, the iodine atom in the dissolution process is almost an inert spectator, playing an insignificant role in the subsequent dynamics in which the excess-electron water cluster undergoes the rearrangement with the high *KE* arisen from the I•···H repulsion. This high *KE* is quickly distributed to the H atoms within 50 fs, and so the directional momentum in favor of a kinetics-driven structure would not play a significant role in the reconstruction of the water network. The ES-AIMD simulations of $I^-(H_2O)_{n=2-4}$ show that the resulting structures are of the lowest energy structures because both the global minimum energy structures and the minimum free energy structures are equivalent. However, in the ES-AIMD simulations of $I^-(H_2O)_5$ with $KE_0 = 100-400$ K, the resulting excess-electron water clusters are not necessarily the same with the global minimum energy structures at 0 K but reflect the entropy-driven structures which can be obtainable at high temperatures.

Here, we have shown that the iodine plays an important role for the first 20−30 fs of MD simulations. Upon excitation, the electron is immediately transferred from the iodine anion to the water cluster [in the case of $I^-(H_2O)_4$ complex, the electron is delocalized over the water tetramer ring]. In the beginning, the *KE* of H atoms grows rapidly so that the reorientation of H atoms occurs without breaking the H-bonds due to the slow motion of the O atoms. However, the duration of this effect due to the I•···H repulsion is very short (20−30 fs), so the overall water network hardly changes except for the orientation of the H atoms adjacent to the iodine radical. During this short period, the cluster has gotten high initial kinetic energy. At the early stage of MD simulations, the I•···H repulsion is important, and so our conclusions are consistent with the argument of Chen and Sheu[25d−f] that iodine plays an important role. However, ∼30 fs after the excitation, the role of the neutral iodine is not significant except that the initial kinetic energy of the cluster increased because the duration of the I•···H repulsion is very short. After the iodine radical is released, the solvent molecules with some high *KE* rearrange, which is consistent with the "solvent-driven" model proposed by Neumark.[1] Thus, both the important role of the iodine and the spectator role of the iodine in the dissolution dynamics are considered correct but not complete. Nevertheless, during the first 20−30 fs, only the H orientations rapidly change, whereas the water network hardly changes. Thus, the overall picture seems to be more consistent with the solvent-driven model.

Concluding Remarks

Although there have been numerous theoretical studies on solvation/hydration, no serious studies on dissolution/dehydration phenomena are available. In this study, we have shown the excited-state molecular dynamics for the CTTS-driven dissolution/dehydration phenomena. By carrying out ES-AIMD simulations for $I^-(H_2O)_{n=2-5}$ complexes, we investigated the time evolution of conformations, NBO charges, interatomic distances, and *KE*s of $I^-(H_2O)_{n=2-5}$ clusters. Our study demonstrates how the detachment process of $I^-(H_2O)_{n=2-5}$ evolves after the excitation and why the evolution process of $I^-(H_2O)_5$ is different from other smaller sizes of clusters $I^-(H_2O)_{2-4}$. To reproduce experimental VDE values for $I^-(H_2O)_5$, it was necessary to perform ES-AIMD simulations at higher temperatures. The present ES-AIMD study gives an insight into the mechanism of the dehydration/dissolution phenomena of iodine atoms and the rearrangement process of the excess-electron water clusters by photoexcitation. $I^-(H_2O)_{n=2-4}$ show simple population decays because the minimum free energy structures around 300 K are equivalent to the global minimum energy structures at 0 K. On the other hand, $I^-(H_2O)_{n=5}$ exhibits the entropy-driven dynamics because the minimum free energy structures (i.e., linear structure) around 100−300 K are different from the minimum energy structures at 0 K.

Both the important role of iodine and the spectator role of iodine in the dissolution dynamics are considered correct but not complete. Meanwhile, the overall picture seems to be more consistent with the solvent-driven model.

Finally, it should be also noted that the present dynamics is important for the design of novel dynamic receptors which can selectively bind ions and then release them by the CTTS mechanism upon excitation. This concept would open a new field of the dynamic host−guest chemistry involved in the capture−transport−release mechanism of smart receptors.

Acknowledgment. This work was supported by GRL (KICOS) and BK21 (KRF). Calculations were carried out by using supercomputers at KISTI.

JA072427C